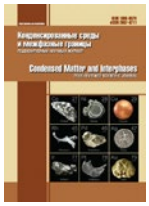

ISSN 1606-867X (Print)
ISSN 2687-0711 (Online)
Condensed Matter and Interphases
Kondensirovannye Sredy i Mezhfaznye Granitsy
https://journals.vsu.ru/kcmf/

Original articles

Research article
https://doi.org/10.17308/kcmf.2026.28/13971

Study on the efficiency of laser radiation attenuation using a nickel phthalocyanine-based nanocomposite with cyclotriphosphazene substituent and single-walled carbon nanotubes

M. S. Savelyev[1,2]✉, P. N. Vasilevsky[1], E. P. Otsupko[1], A. Yu. Tolbin[3], A. Yu. Gerasimenko[1,2]

[1]National Research University of Electronic Technology,
1, Shokin sq., Zelenograd, Moscow 124498, Russian Federation

[2]I. M. Sechenov First Moscow State Medical University,
8-2, Trubetskaya st., Moscow 119991, Russian Federation

[3]Institute of Physiologically Active Compounds at Federal Research Center of Problems of Chemical Physics and Medicinal Chemistry of the Russian Academy of Sciences,
1, Severny proezd, Chernogolovka 142432, Russian Federation

Abstract

Objectives: A key challenge in nonlinear optics is the development of high-performance materials for optical limiters of laser radiation. Such materials must combine high linear transmittance under low-intensity irradiation—ensuring efficient transmission of the useful optical signal—with fast, reversible switching to an opaque state once the intensity threshold is exceeded, thereby providing protection against nanosecond-duration pulses. Meeting these requirements is essential for safeguarding sensitive optoelectronic components, such as charge-coupled devices (CCDs), complementary metal-oxide-semiconductor (CMOS) structures, and other detection systems. A promising candidate to address this challenge is a nanocomposite that integrates single-walled carbon nanotubes (SWCNTs) with nickel phthalocyanine molecules functionalized by a cyclotriphosphazene substituent.

Experimental: The nonlinear optical properties of the synthesized nanocomposite were evaluated using the open aperture Z-scan method. A 1070 nm ytterbium fiber laser was used as the radiation source, generating 4 ns pulses with a repetition rate of 50 kHz at an average power of 550 mW. A comparative analysis of the nonlinear response was performed for three samples dispersed in dimethylformamide (DMF): a solution of tert-butyl-substituted nickel phthalocyanine with a cyclotriphosphazene moiety (1 – NiPct-ppz), an SWCNT dispersion (2), and a hybrid dispersion based on the proposed nanocomposite (3 – NiPct-ppz@SWCNT). A quantitative assessment of the confinement efficiency for each sample was performed using the CORRELATO algorithm, the methodology of which was described in our previous studies. The input parameters for the algorithm were determined based on a mathematical model grounded in the radiation transfer equation and accounting for the threshold nature of the nonlinear optical response.

Conclusions: According to the results of a comprehensive evaluation conducted using the CORRELATO algorithm, nanocomposite 3 demonstrated the greatest effectiveness in attenuating laser radiation. The synergistic effect in the hybrid is due to the combination of the properties of the constituent components: a low nonlinearity threshold characteristic of the phthalocyanine complex ($F_x \approx 0.12$ J/cm^2), and the mechanism of additional nonlinear scattering introduced by carbon nanotubes. As a result of hybridization, a significant increase in the nonlinear absorption coefficient was achieved, with a value exceeding 480 cm/GW for the composite.

Keywords: Laser radiation limiters, Carbon nanotubes, Phthalocyanines, Z-scan, Radiation transfer equation, Nonlinear absorption, Nonlinear refraction, CORRELATO

Funding: The research was carried out with the financial support of the Russian Science Foundation (Grant 25-73-20034).

✉ Mikhail Savelyev, t1004380@org.miet.ru
© Savelyev M. S., Vasilevsky P. N., Otsupko E. P., Tolbin A. Yu., Gerasimenko A. Yu., 2026

The content is available under Creative Commons Attribution 4.0 License.

For citation: Savelyev M. S., Vasilevsky P. N., Otsupko E. P., Tolbin A. Yu., Gerasimenko A. Yu. Study on the efficiency of laser radiation attenuation using a nickel phthalocyanine-based nanocomposite with cyclotriphosphazene substituent and single-walled carbon nanotubes. *Condensed Matter and Interphases*. 2025;27(3): 425–435. https://doi.org/10.17308/kcmf.2026.28/13971

Оригинальные статьи

Научная статья
УДК 538.958
Научная специальность ВАК – 1.3.8. Физика конденсированного состояния
https://doi.org/10.17308/kcmf.2026.28/13971

Исследование эффективности ограничения лазерного излучения нанокомпозитом на основе фталоцианина никеля с циклотрифосфазеновым заместителем и однослойных углеродных нанотрубок

М. С. Савельев[1,2]✉, П. Н. Василевский[1], Е. П. Оцупко[1], А. Ю. Толбин[3], А. Ю. Герасименко[1,2]

[1]Национальный исследовательский университет «Московский институт электронной техники», пл. Шокина, 1, Зеленоград, Москва 124498, Российская Федерация

[2]Первый Московский государственный медицинский университет имени И. М. Сеченова, ул. Трубецкая, 8-2, Москва 119991, Российская Федерация

[3]Институт физиологически активных веществ Федерального исследовательского центра проблем химической физики и медицинской химии Российской академии наук, Северный проезд, 1, Черноголовка 142432, Российская Федерация

Аннотация

Цель статьи: Ключевой задачей в области нелинейной оптики является разработка материалов с повышенной эффективностью для оптических ограничителей лазерного излучения. Подобные материалы должны обладать высоким линейным пропусканием в условиях низкоинтенсивного облучения, обеспечивая передачу полезного оптического сигнала, и одновременно демонстрировать быстрое и обратимое переключение в непрозрачное состояние при превышении порога интенсивности, обеспечивая защиту от импульсов наносекундной длительности. Реализация данных требований позволяет обеспечить сохранность высокочувствительных оптико-электронных компонентов, включая приборы с зарядовой связью (ПЗС), комплементарные структуры металл-оксид-полупроводник (КМОП) и иные детектирующие системы. В качестве перспективного материала для решения указанной задачи предлагается нанокомпозит, интегрирующий молекулы фталоцианина никеля, функционализированного циклотрифосфазеновым заместителем, и однослойные углеродные нанотрубки (ОУНТ).

Экспериментальная часть: Оценка нелинейно-оптических свойств синтезированного нанокомпозита проводилась методом Z-сканирования в режиме открытой апертуры. В качестве источника излучения использовался волоконный лазер на иттербии с длиной волны 1070 нм, генерирующий импульсы длительностью 4 нс с частотой повторения 50 кГц при средней мощности 550 мВт. Сравнительный анализ нелинейного отклика проводился для трех образцов, диспергированных в диметилформамиде (ДМФА): раствор *трет*-бутил замещенного фталоцианина никеля с циклотрифосфазеновым фрагментом (**1** – NiPc^t-ppz), дисперсия ОУНТ (**2**) и гибридная дисперсия на основе предложенного нанокомпозита (**3** – NiPc^t-ppz@ОУНТ). Количественная оценка эффективности ограничения для каждого образца выполнялась с использованием алгоритма CORRELATO, методология которого была описана в наших предыдущих исследованиях. Определение входных параметров для алгоритма осуществлялось на основе математической модели, базирующейся на уравнении переноса излучения и учитывающей пороговую природу нелинейно-оптического отклика.

Выводы: По результатам комплексной оценки, проведенной алгоритмом CORRELATO, нанокомпозит **3** продемонстрировала наибольшую эффективность ограничения лазерного излучения. Синергетический эффект в гибриде обусловлен комбинацией свойств исходных компонентов: низкого порога нелинейности, характерного для фталоцианинового комплекса ($F_x \approx 0.12$ Дж/см^2), и механизма дополнительного нелинейного рассеяния, вносимого углеродными нанотрубками. В результате гибридизации достигнуто существенное увеличение нелинейного коэффициента поглощения, значение которого для композита превысило 480 см/ГВт.

Ключевые слова: ограничители лазерного излучения, углеродные нанотрубки, фталоцианины, Z-сканирование, уравнение переноса излучения, нелинейное поглощение, нелинейное преломление, CORRELATO

✉ Савельев Михаил Сергеевич, e-mail: t1004380@org.miet.ru

© Савельев М. С., Василевский П. Н., Оцупко Е. П., Толбин А. Ю., Герасименко А. Ю., 2026

Источник финансирования: Работа выполнена при финансовой поддержке РНФ (грант № 25-73-20034).
Для цитирования: Савельев М. С., Василевский П. Н., Оцупко Е. П., Толбин А. Ю., Герасименко А. Ю. Исследование эффективности ограничения лазерного излучения нанокомпозитом на основе фталоцианина никеля с циклотрифосфазеновым заместителем и однослойных углеродных нанотрубок. *Конденсированные среды и межфазные границы*. 2026;28(3): 425–435. https://doi.org/10.17308/kcmf.2026.28/13971

1. Introduction

The development of effective passive laser protection for light-sensitive devices, including CCD and CMOS cameras, as well as other detection systems – remains a critical scientific challenge [1–3]. A key requirement for such protective materials is high transmission of the operational optical signal combined with the ability to sharply attenuate high-intensity radiation. This capability is essential for the reliable operation of high-performance optical components used in powerful laser systems, particularly in space applications where both high pulse repetition rates and continuous-wave operation are required. Damage to these components reduces their service life in applications such as laser ranging, gravitational wave detection, and space lidar sounding [4]. Traditional colored optical filters are of limited use because they attenuate harmful and useful signals uniformly, preventing devices from operating in normal mode [5]. Furthermore, systems operating in the spectral range around 1 μm with nanosecond pulses and various repetition rates are widely used [6]. Accordingly, this study investigated the attenuation of laser radiation at a wavelength of 1070 nm, with a pulse duration of 4 ns and a repetition rate of 50 kHz.

A number of materials exhibiting nonlinear optical properties have already been proposed for the near-infrared range [7, 8]. Nevertheless, there remains a need to improve the efficiency of optical confinement of high-power laser radiation [9]. Among promising materials, phthalocyanines stand out due to their structural stability, even under intense femtosecond pulses [10, 11]. Carbon nanotubes are also noteworthy, as they outperform other allotropic forms of carbon through a combination of absorption and scattering [12]. Improving efficiency requires consideration of the specific characteristics of these materials. For phthalocyanines, the molecular structure is of key importance [13–16], as it determines their optical properties and can be modeled using quantum-chemical methods [9, 17]. Among carbon nanomaterials, single-walled carbon nanotubes (SWCNTs) are the most promising [18]. Although their optical properties may be similar to those of multi-walled nanotubes [11, 19], the functionalization of SWCNTs allows for more effective modification of their nonlinear characteristics. This is due to the inability of the dye to interact with the inner walls of multi-walled nanotubes. It is known that the formation of nanostructures involving nanotubes is carried out primarily in two ways: by binding to the outer walls [11, 18–20] or by filling the inner cavity with dye molecules, which is achievable in the presence of open ends and a certain diameter of the nanotubes [21].

The degree of nanotube dispersion plays a significant role, as nanotubes may exist as agglomerates, clusters, or individually dispersed species [22]. This factor affects the efficiency of functionalization and can limit the magnitude of the nonlinear optical response [23]. In this work, we investigated

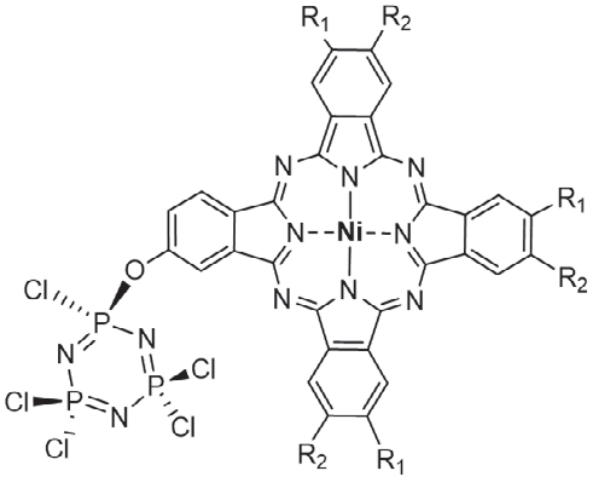

1

R_1/R_2 = H / *tert*-butyl

Fig. 1. Chemical structure of phthalocyanine 1

nanostructures composed of a previously synthesized tert-butyl-substituted nickel phthalocyanine bearing a cyclotriphosphazene substituent (1), whose structure was examined using quantum chemical modeling [9], and CNTs dispersed in dimethylformamide (DMF) using an immersion ultrasound homogenizer, a method that ensures optimal dispersion of the nanotubes [23].

Functional groups can have a significant effect on particle agglomeration [24, 25]. A similar effect was observed during the covalent attachment of phthalocyanines with various central metal atoms [5]. Surfactants can be used to suppress agglomeration [26, 27], especially in cases where the synthesized material retains a tendency to aggregate. In this work, Triton X-100 was used as the surfactant.

In this regard, our paper is devoted to the development and comprehensive study of a hybrid nanomaterial based on functionalized nickel phthalocyanine and single-walled carbon nanotubes (NiPct-ppz@SWCNT) for the creation of effective optical limiters in the near-infrared range. The main focus will be on a systematic study of its nonlinear optical characteristics using the Z-scan method under conditions simulating the actual operating conditions of optical limiters. A mathematical model that adequately describes the effectiveness of optical limiting, obtained using the CORRELATO method, has been validated. This research contributes to solving the fundamental problem of creating materials with controllable nonlinear optical properties to protect optoelectronic devices from high-power laser radiation.

2. Materials and methods

2.1. Materials

Three dispersions were prepared in N,N-dimethylformamide (DMF): nickel phthalocyanine (concentration ~ $1.5 \cdot 10^{-4}$ M), functionalized with a cyclotriphosphazene moiety (sample 1); single-walled carbon nanotubes (SWCNTs) (Tuball, Luxembourg) (concentration ~ 0.002 wt. %), stabilized with the surfactant Triton X-100 (sample 2); a nanostructured complex based on nickel phthalocyanine (with a cyclotriphosphazene moiety) (concentration ~ $1.5 \cdot 10^{-4}$ M) and CNTs (concentration ~ 0.002 wt. %), stabilized with the surfactant Triton X-100 (sample 3).

The Tuball nanotubes used had the following characteristics: a purity of at least 99 wt. %, a content of other allotropic forms of carbon and metallic impurities of less than 1 wt. %, an average diameter of ~1.6 nm, a length of over 5 μm, and a specific surface area of ≈ 1000 m^2/g [28]. Dispersions with nanotubes (samples **2** and **3**) were prepared using a Soniqator Q700 immersion ultrasonic homogenizer (QSonica, USA) (20 kHz, 280 W) for 2 hours. To prevent overheating, the process was carried out in a water-cooled bath, maintaining the reaction mixture temperature at no higher than 40 °C. Spectral measurements of the obtained samples in DMF were performed on a GENESYS 10S spectrophotometer (Thermo Fisher Scientific, USA).

The resulting dispersions exhibit high resistance to intense laser radiation, ensuring the stability of their linear optical properties. The use of unseparated SWCNTs with mixed chirality allows for a broadband optical response in the near-IR region of the spectrum at a controlled concentration [29]. Covalent attachment of phthalocyanine complexes to the surface of nanotubes, combined with the use of surfactants, helps reduce the tendency of SWCNTs to agglomerate and increases the long-term stability of the dispersions.

2.2. Open aperture Z-scan method

Nonlinear optical experiments were conducted using the setup shown in Fig. 2. An ytterbium laser with the following parameters was used as the radiation source: average power – 550 mW, pulse repetition rate – 50 kHz, pulse duration – 4 ns. The power of the incident radiation was adjusted using a polarization attenuator consisting of a fixed polarizer and a rotating Glan-Taylor prism (Standa, Lithuania). After attenuation, the laser beam was focused by a lens. The Rayleigh length was ~0.1 cm. Variations in power density (exposure) on the sample were achieved by moving it along the optical axis (Z) using a motorized stage. The position of the focal plane was taken as the origin (Z = 0). The sample, placed in a 0.1 cm thick quartz cuvette, was moved in the range from

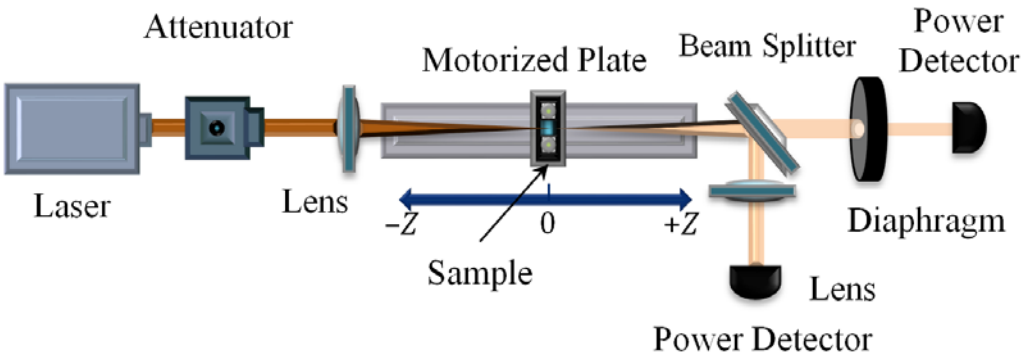

Fig. 2. Experimental setup for determining optical characteristics using the Z-scan method

$-z_{max}$ to $+z_{max}$ relative to the focus. To record the data, a portion of the radiation passing through the sample was deflected by a beam-splitter, collimated by a second lens, and recorded by a power detector. The nonlinear absorption coefficient was determined by approximating the experimental dependence of the normalized transmittance on the sample position (Z-scan). The linear absorption coefficient was measured with the sample positioned far from the focal plane, where the influence of nonlinear effects is negligible.

2.3. Closed aperture Z-scan

To determine the nonlinear refractive index, closed aperture Z-scan was performed. The normalized transmittance with the closed aperture was corrected by dividing it by the curve obtained in the open aperture mode to eliminate the contribution of nonlinear absorption. The nonlinear refractive index was calculated using the standard Z-scan method; the linear refractive index was measured using a refractometer.

3. Theory

3.1. Open aperture Z-scan

The nonlinear absorption coefficient was determined using the radiation transfer equation [5]:

$$\int_{I_0}^{I} \frac{1}{I\mu(I)} dI = -d. \quad (1)$$

In equation (1), I is the output intensity, I_0 is the incident intensity, μ is the absorption coefficient, and d is the layer thickness. In the case of intensity-dependent absorption, the coefficient is a function of I (taking into account the threshold intensity I_x and the nonlinear contribution β along with the linear component α):

$$\mu(I) = \alpha + \beta(I - I_x)\eta(I - I_x). \quad (2)$$

In equation (2), α is the linear absorption coefficient (cm^{-1}), β is the nonlinear absorption coefficient (cm/GW), and I_x is the threshold laser intensity (J/cm^2). Assuming a uniform distribution of radiation intensity throughout the material, the absorption coefficient can be considered constant, which holds true for homogeneous systems. For a beam with a "flat-top" profile, the expression for normalized transmittance is obtained by substituting equation (2) into equation (1):

$$T_n(z) = \exp\left(-\frac{2\beta}{\pi^{3/2}\nu\tau w^2(z)}(P_0 - P_x)d\right). \quad (3)$$

In equation (3), ν is the pulse repetition frequency (Hz), τ is pulse duration (ns), w is the beam radius (μm), which depends on the z-offset for Z-scan method, the focal radius is w_0, and the Rayleigh length z_0:

$$w^2(z) = w_0^2\left(1 + \frac{z^2}{z_0^2}\right). \quad (4)$$

In equation (3), the incident and threshold powers are denoted as P_0 and P_x. These parameters are used to determine the intensity in equations (1) and (2) using the following expression:

$$I = \frac{2P}{\pi^{3/2}\nu\tau w^2}. \quad (5)$$

The attenuation capability is characterized by the attenuation coefficient (D_P) and is determined by the ratio of output power to input power:

$$D_P = 10\lg\left(\frac{P_0}{P_{out}}\right). \quad (6)$$

In equation (6), P_{out} is the transmitted power. The analytical expression (3) for the normalized transmittance, based on the selected nonlinear absorption model, is used to approximate the experimental curves.

3.2. Closed aperture Z-scan

The nonlinear refractive index n_n was determined from the normalized transmission curve obtained with the closed aperture, taking into account a correction for the open aperture (to exclude the contribution of nonlinear absorption) [30]. The value of n_n was calculated from the shape and amplitude of the corrected curve using the following formula:

$$T_n(x) = 1 - \frac{16 n_n P_0 \left(1 - \exp(-\alpha d)\right) x}{\lambda \nu \tau w^2 \alpha \sqrt{\pi}\left(x^2+9\right)\left(x^2+1\right)}. \quad (7)$$

In expression (7), $x = z/z_0$ is the normalized coordinate, where λ is the wavelength of the laser radiation (nm).

3.3. Study on the optical limiting

The performance of the optical limiter was evaluated based on a set of parameters: linear absorption coefficient α, nonlinear absorption coefficient β, dynamic range DR, exposure threshold F_x, and attenuation coefficient D_P. For their comprehensive evaluation, correlation relationships were applied that were previously developed using the CORRELATO algorithm and validated in our work [5]. The descriptors σ_1 and σ_2 were introduced:

$$\sigma_1 = \lg\left(\beta^{-1}\alpha^{-2}\right), \quad (8)$$

$$\sigma_2 = 10^{\frac{D_P}{10}} \frac{\beta}{DR \cdot F_x}. \quad (9)$$

The parameter σ_1, determined from expression (8), characterizes the negative effect of aggregation on the efficiency of the limiting process. The further the value is shifted into the negative region, or the smaller it is, the smaller the negative contribution of aggregation to optical limiting [31]. Meanwhile, σ_2 reflects the total optical nonlinearity (the model was trained on quantum-chemical data) and should have the maximum possible value to improve the properties of the potential limiter [32].

Dynamic range and exposure threshold are defined by the following relationships:

$$DR = \frac{P_0}{P_x}, \quad (10)$$

$$F_x = \frac{2P_x}{\pi \nu w_0^2}. \quad (11)$$

The relationship between the descriptors σ_1 and σ_2 is analyzed on a double-logarithmic scale (a plot of θ_2 versus θ_1):

$$\theta_1 = \lg(\sigma_2), \quad (12)$$

$$\theta_2 = \lg\left(\sigma_1^2 \sigma_2^2\right). \quad (13)$$

The calculated values should have a linear relationship.

4. Experimental

Figure 3 shows the normalized optical density spectra of all the samples studied. The normalization was performed relative to the maximum of the absorption band (Q-band). The absorption bands characteristic of the

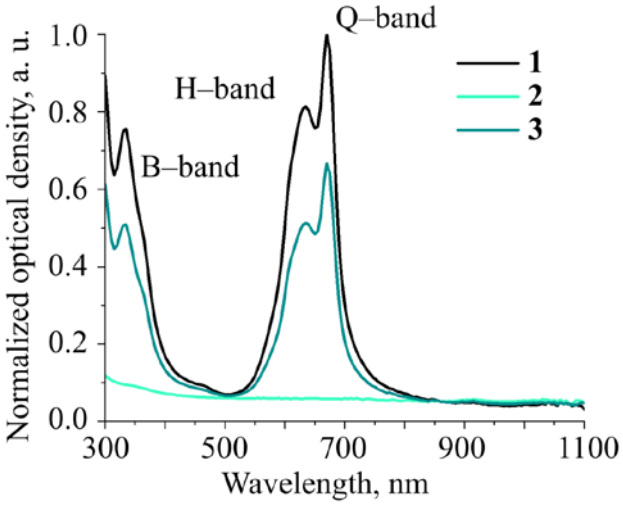

Fig. 3. Spectrum of normalized optical density of samples

phthalocyanine chromophore – the B-band (Soret) and the Q-band – are clearly identifiable in the spectra.

Figure 4a shows the dependence of normalized transmittance on the sample's position relative to the focal plane (Z-scan), obtained using open aperture Z-scan. The minimum value of normalized transmittance is observed for sample **3**. Samples **1** and **2**, consisting of individual components of the nanocomposite (sample **3**), exhibit a less pronounced nonlinear optical response, as evidenced by higher minimum values on their curves. The experimental data are approximated by theoretical curves calculated using equation 3.

Figure 4b shows the dependence of normalized transmittance on the sample position, obtained by dividing the curves measured in the closed-aperture and open-aperture modes. The nonlinear refractive index was calculated using equation (7). The greatest change in the refractive index is observed for sample **3** and significantly exceeds the values obtained for samples **1** and **2**, indicating synergistic enhancement of the nonlinear response in the nanocomposite. For quantitative analysis, the nonlinear optical parameters of the materials (two-photon absorption coefficient, nonlinear refraction) were calculated and are presented in Table 1.

5. Results and discussion

The optical characteristics of all three samples are summarized in Table 1. Scanning along the Z-coordinate was performed within a sample displacement range of –1 to +1 cm. Correlation analysis was performed using equations (8), (9), (12), and (13) after substituting the values with the dimensions specified in the table.

Figure 5 shows the distribution of nonlinear absorbers across different zones. The division into regions and the selection of a "middle ground" are arbitrary, but they greatly facilitate the visual interpretation of the data. Analysis based on the σ_1 and σ_2 descriptors allows us to identify sample **3**, which is characterized by the highest values of both descriptors. This may be due to energy transfer between phthalocyanine (electron donor) and the nanotube (acceptor) [33, 34]. Efficient charge transfer opens up prospects for improving optical confinement. In the case of samples **1** and **2**, assessing their efficiency is less straightforward. To resolve this uncertainty, a double-logarithmic scale was applied (Fig. 6). If a material falls into the range of negative values for θ_1 and θ_2, its practical properties are likely insufficient, and the material itself is classified as belonging to the "weak" range [5]. No such materials were identified during the study. Thus, samples **1** and **2** were classified as belonging to

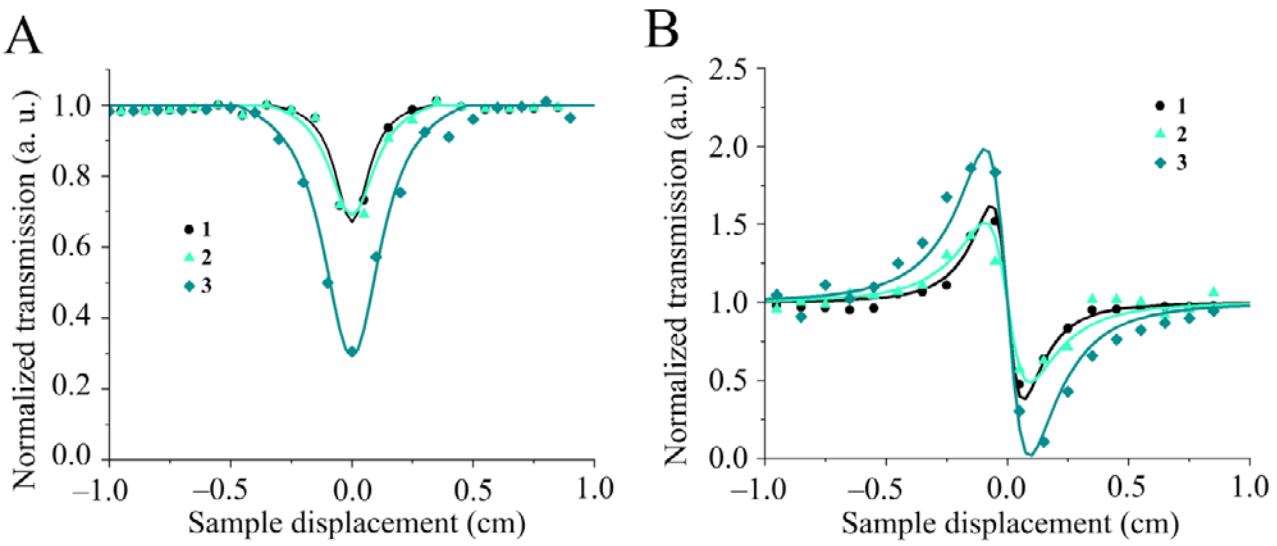

Fig. 4. Z-scan experiment data: open aperture (a); data from closed aperture divided by data from open aperture (b)

Table 1. Optical parameters of the manufactured dispersions

Characteristic	Sample		
	1	**2**	**3**
Input power (P_0), mW	544	541	540
Linear absorption coefficient (α), cm^{-1}	1.9	1.7	2.0
Nonlinear absorption coefficient (β), cm/GW	110	150	480
Radius of the beam waist (w_0), μm	16	19	19
Peak intensity (I_0), GW/cm^2	0.15	0.11	0.11
Threshold fluence (F_x), J/cm^2	0.12	0.16	0.12
Linear refractive index (n_0)	1.4272	1.4270	1.4278
Nonlinear refractive index (n_n), cm^2/TW	1.5	1.9	4.0
Attenuation coefficient (D_p), dB	2.6	2.1	5.7
Dynamic range (*DR*)	21.8	12.0	15.4
σ_1	2.60	2.64	3.28
σ_2	74	127	936
θ_1	1.87	2.11	2.97
θ_2	4.57	5.05	6.98

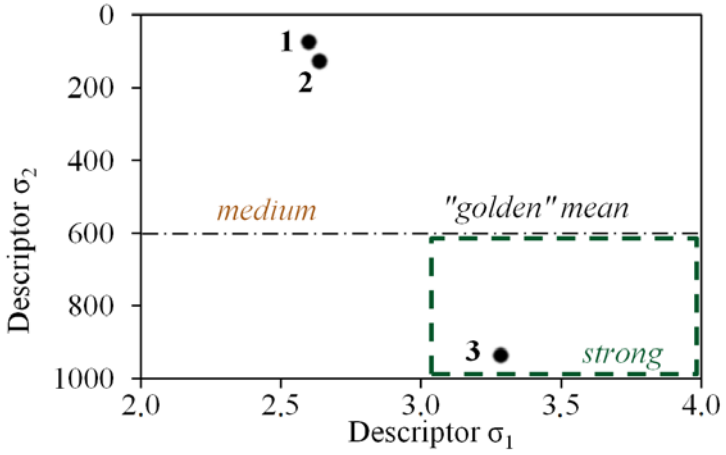

Fig. 5. Dependence of the values of the descriptor σ_2 on the descriptor σ_1

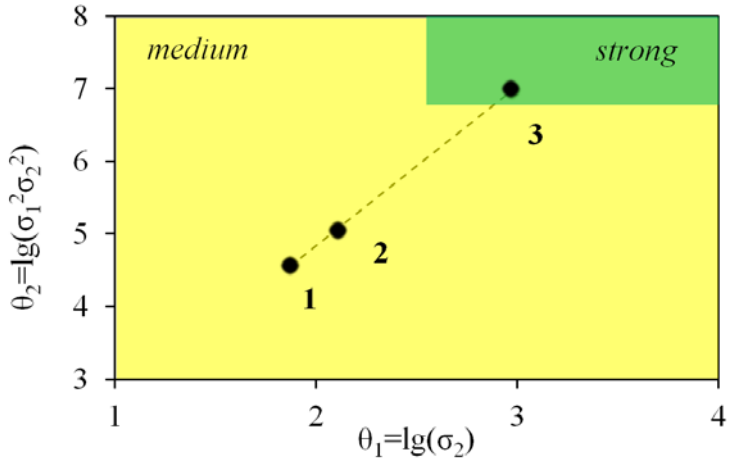

Fig. 6. Evaluation of the reliability of the results of correlation analysis on a double logarithmic scale (θ_2 *vs* θ_1)

the "medium" range, and sample **3** to the "strong" range.

The following main results were obtained:

– The highest value of the nonlinear absorption coefficient (480 cm/GW) was recorded for sample **3**, which also exhibits a high value of the nonlinear refractive index;

– The lowest power threshold is observed for sample **1**;

– According to the boundary conditions for the descriptors σ_1 and σ_2, sample **3** belongs to the "strong" range;

– Samples **1** and **2** fall in the middle range in terms of effectiveness and belong to the "medium" range;

– In a bilogarithmic analysis, all data points form a linear relationship, confirming the suitability of the model used to describe them.

The present study leads to the following conclusions. Sample **3** demonstrated the highest efficiency and the best attenuation characteristics for high-power laser radiation, as well as a low threshold exposure value compared to sample **1**, which is primarily due to the structure of the phthalocyanine [15, 16]. The dynamic range for sample **3** is due to the large beam radius (related to different focusing within the material) resulting from focusing. It led to a reduction in the maximum laser radiation exposure during the experiments at similar power levels. This indicates the potential for its practical application as an effective nonlinear optical limiter for the creation of high-speed optical devices. An important task is to control scattering in samples **2** and **3**, which contain SWCNTs, since it contributes to the overall attenuation. Samples **1** and **2**, while exhibiting similar properties, are significantly inferior to sample **3** in terms of efficiency, which led to their classification in the "medium" range. At the same time, energy transfer between phthalocyanine and the nanotube affected virtually all characteristics except for the threshold exposure.

Authors' contributions

M. S. Savelyev – original draft, theoretical model, conclusions. P. N. Vasilevsky – experimental data analysis, methodology, text editing. Otsupko E. P. – data collection. Tolbin A. Yu. – research concept, theoretical model, text editing. Gerasimenko A. Yu. – scientific supervision, text editing.

Conflict of interests

The authors declare that they have no known competing financial interests or personal relationships that could have influenced the work reported in this paper.

References

1. Lv X., Pan Y., Jia Z., Li Z., Ni X. Surface damage induced by a combined millisecond and nanosecond laser. *Applied Optics*. 2017;56: 5060. https://doi.org/10.1364/AO.56.005060

2. Westgate C., James D. Visible-band nanosecond pulsed laser damage thresholds of silicon 2D imaging arrays. *Sensors*. 2022;22: 2526. https://doi.org/10.3390/s22072526

3. Jian Z., Zhou W., Chang H., Ma Y., Quan X., Wang Z. Thermal damage characterization of detector induced by nanosecond pulsed laser irradiation. *Photonics*. 2025;12: 790. https://doi.org/10.3390/photonics12080790

4. Pan Q., Wang K., Han J., Ma B. Damage dynamics and relaxation process of double pulses with nanosecond laser. *Photonics Research*. 2025;13: 2246. https://doi.org/10.1364/PRJ.539648

5. Savelyev M. S., Vasilevsky P. N., Dudin A. A., Tolbin A. Yu., Pavlov A. A., Gerasimenko A. Yu. Optical limiting properties of composites of iron, nickel and cobalt phthalocyanine complexes with single-wall carbon nanotubes and assessment of their efficiency by latest correlation methods. *Technical Physics*. 2025;70(5): 909. https://doi.org/10.61011/TP.2025.05.61129.443-24

6. Bi W., Meng Y., Wang Y., … Liu H. Failure mechanisms of a silicon-based CMOS image sensor irradiated by a 1550 nm nanosecond laser. *Optics Express*. 2024;32: 4709. https://doi.org/10.1364/OE.515728

7. Kawya J., Girisun T. C. S. Upconversion enabled optical limiting behaviour in Y_2O_3: Yb, Er nanophosphors under 532 nm and 1064 nm laser excitation. *Journal of Luminescence*. 2025;277: 120903. https://doi.org/10.1016/j.jlumin.2024.120903

8. Stavrou M., Papadakis I., Bawari S., Narayanan T. N., Couris S. Giant broadband (450–2300 nm) optical limiting and enhancement of the nonlinear optical response of some graphenes by defect engineering. *The Journal of Physical Chemistry C*. 2021;125: 16075–16085. https://doi.org/10.1021/acs.jpcc.1c05495

9. Tolbin A. Y., Savelyev M. S., Vasilevsky P. N., Gerasimenko A. Y. Conditions for the efficiency of optical limiting based on experiment and quantum chemical calculations. *Physical Chemistry Chemical Physics*. 2024;26: 8965–8972. https://doi.org/10.1039/D4CP00055B

10. Xiao Z., Shi Y., Sun R., … Song Y. Ultrafast broadband optical limiting in simple pyrene-based molecules with high transmittance from visible to infrared regions. *Journal of Materials Chemistry C*. 2016;4: 4647–4653. https://doi.org/10.1039/C5TC04047G

11. Venkatram N., Narayana Rao D., Giribabu L., Venugopal Rao S. Femtosecond nonlinear optical properties of alkoxy phthalocyanines at 800 nm studied using Z-scan

technique. *Chemical Physics Letters*. 2008;464: 211–215. https://doi.org/10.1016/j.cplett.2008.09.029

12. Tolbin A. Y., Tretyakov B. A., Savelyev M. S., Vasilevsky P. N., Gerasimenko A. Y. Intelligent methods for assessing the efficiency of optical limiters based on carbon nanomaterials using the CORRELATO approach. *Physical Chemistry Chemical Physics*. 2025;27: 18467–18477. https://doi.org/10.1039/D5CP02157J

13. de la Torre G., Vázquez P., Agulló-López F., Torres T. Role of structural factors in the nonlinear optical properties of phthalocyanines and related compounds. *Chemical Reviews*. 2004;104: 3723–3750. https://doi.org/10.1021/cr030206t

14. Ou C., Lv W., Chen J., ... Yang G. Structural, photophysical and nonlinear optical limiting properties of sandwich phthalocyanines with different rare earth metals. *Dye and Pigments*. 2021;184: 108862. https://doi.org/10.1016/j.dyepig.2020.108862

15. Kuzmina E. A., Dubinina T. V., Tomilova L. G. Recent advances in chemistry of phthalocyanines bearing electron-withdrawing halogen, nitro and N-substituted imide functional groups and prospects for their practical application. *New Journal of Chemistry*. 2019;43: 9314. https://doi.org/10.1039/C9NJ01755K

16. Kuzmina E. A., Dubinina T. V., Vasilevsky P. N., ... Tomilova L. G. Novel octabromo-substituted lanthanide(III) phthalocyanines – prospective compounds for nonlinear optics. *Dyes and Pigments*. 2021;185: 108871. https://doi.org/10.1016/j.dyepig.2020.108871

17. Samawi K. A., Imad Ali S., Salman T. A., Alshekhly B. A. Exploring the capabilities of metal-doped phthalocyanine (MPC, M = Co, Cu, Fe, Ni, Zn) for adsorption of CO_2: a DFT study. *Journal of Molecular Graphics and Modelling*. 2025;140: 109088. https://doi.org/10.1016/j.jmgm.2025.109088

18. Gowda P. B. R., Bhovi V. K., Hegde S. N., ... Kariduraganavar M. Y. Enhanced optoelectronic properties of single-walled carbon nanotubes via functionalization with pyridine-based Y-shaped chromophores. *Carbon N. Y.* 2025;245: 120744. https://doi.org/10.1016/j.carbon.2025.120744

19. Mathew R. J., Chandran A. R., Kishor K. S. S., Joseph L. K., Saji K. J., Sajeev U. S. Tunable nonlinear optical properties in polyaniline-multiwalled carbon nanotube (PANI-MWCNT) system probed under pulsed Nd:YAG laser. *Next Materials*. 2025;*6*: 100431. https://doi.org/10.1016/j.nxmate.2024.100431

20. Elwekeel W. M., Salah A., Ismail T., ... Anis B. Superior nonlinear optical and optical limiting properties of cross-linked and thermally stable HiPCO-SWCNTs@PVA films. *Optical Materials*. 2021;122: 111732. https://doi.org/10.1016/j.optmat.2021.111732

21. Gonzalez-Muñoz D., Martin-Somer A., Strobl K., ... Aleman J. Enhancing visible-light photocatalysis via endohedral functionalization of single-walled carbon nanotubes with organic dyes. *ACS Applied Materials & Interfaces*. 2021;13: 24877–24886. https://doi.org/10.1021/acsami.1c04679

22. Wang S., Liang Z., Wang B., Zhang C., Rahman Z. Precise cutting of single-walled carbon nanotubes. *Nanotechnology*. 2007;18: 055301. https://doi.org/10.1088/0957-4484/18/5/055301

23. Vasilevsky P. N., Savelyev M. S., Tolbin A. Y., ... Gerasimenko A. Y. Nonlinear optical response of dispersed medium based on conjugates single-walled carbon nanotubes with phthalocyanines. *Photonics*. 2023;10: 537. https://doi.org/10.3390/photonics10050537

24. Benko A., Duch J., Gajewska M., ... Kotarba A. Covalently bonded surface functional groups on carbon nanotubes: from molecular modeling to practical applications. *Nanoscale*. 2021;13: 10152–10166. https://doi.org/10.1039/D0NR09057C

25. Rajendran D., Ramalingame R., Adiraju A., Nouri H., Kanoun O. Role of solvent polarity on dispersion quality and stability of functionalized carbon nanotubes. *Journal of Composites Science*. 2022;6: 26. https://doi.org/10.3390/jcs6010026

26. Metaxa Z. S., Boutsioukou S., Amenta M., Favvas E. P., Kourkoulis S. K., Alexopoulos N. D. Dispersion of multi-walled carbon nanotubes into white cement mortars: the effect of concentration and surfactants. *Nanomaterials*. 2022;12: 1031. https://doi.org/10.3390/nano12061031

27. Yonezawa S., Chiba T., Seki Y., Takashiri M. Origin of n type properties in single wall carbon nanotube films with anionic surfactants investigated by experimental and theoretical analyses. *Scientific Reports*. 2021;11: 5758. https://doi.org/10.1038/s41598-021-85248-9

28. Predtechenskiy M. R., Khasin A. A., Bezrodny A. E., ... Smirnov S. N. New perspectives in SWCNT applications: tuball SWCNTs. Part 1. Tuball by itself—all you need to know about it. *Carbon Trends*. 2022;8: 100175. https://doi.org/10.1016/j.cartre.2022.100175

29. Berciaud S., Cognet L., Poulin P., Weisman R. B., Lounis B. Absorption spectroscopy of individual single-walled carbon nanotubes. *Nano Letters*. 2007;7: 1203–1207. https://doi.org/10.1021/nl062933k

30. Sheik-Bahae M., Said A. A., Wei T.-H., Hagan D. J., Van Stryland E. W. Sensitive measurement of optical nonlinearities using a single beam. *IEEE Journal of Quantum Electronics*. 1990;26: 760–769. https://doi.org/10.1109/3.53394

31. Tolbin A. Yu., Shestov V. I., Savelyev M. S., Gerasimenko A. Yu. Deviation from Beer's law and relationship of aggregation with the effective TPA coefficient: UV-vis studies on a series of low symmetry monophthalocyanines bearing a cyclotriphosphazene substituent. *New Journal of Chemistry*. 2023;47: 1165–1173. https://doi.org/10.1039/d2nj05376d

32. Tolbin A. Yu. An efficient method of searching for correlations between unlimited datasets to provide forecasting models. *Mendeleev Communications*. 2023;33: 419–421, https://doi.org/10.1016/j.mencom.2023.04.038

33. Clavian L. M., Kumar R. P. C., Kumar A. K. V., Narayana Rao D., Shihab N. K., Sanjeev G. Comprehensive analysis on the Z-scan response of thermally evaporated CuTPP thin films in terms of H aggregation and charge transfer dynamics. *The Journal of Physical Chemistry C*. 2024;128: 419. https://doi.org/10.1021/acs.jpcc.3c06473

34. Wang A., Shen X., Wang Q., ... Song Y. Boosted charge transfer in porphyrin and zinc phthalocyanine co-functionalized graphene oxide nanohybrids toward improved optical limiting and H_2 evolution. *Dyes and Pigments*. 2021;187: 109142. https://doi.org/10.1016/j.dyepig.2021.109142

Information about the authors

Mikhail S. Savelyev, Cand. Sci. (Phys.–Math.), Assistant Professor at Institute of Biomedical Systems, National Research University of Electronic Technology – MIET (Zelenograd, Moscow, Russian Federation); Leading Research Fellow, I. M. Sechenov First Moscow State Medical University (Moscow, Russian Federation).

https://orcid.org/0000-0003-1255-0686

t1004380@org.miet.ru

Pavel N. Vasilevsky, Assistant, Engineer in Institute of Biomedical Systems, National Research University of Electronic Technology – MIET (Zelenograd, Moscow, Russian Federation).

https://orcid.org/0000-0002-5733-8497

u130020@edu.miet.ru

Ekaterina P. Otsupko, undergraduate at Institute of Biomedical Systems, National Research University of Electronic Technology – MIET (Zelenograd, Moscow, Russian Federation).

https://orcid.org/0009-0007-8645-4511

8191388@edu.miet.ru

Alexander Yu. Tolbin, Dr. Sci. (Chem.), Professor of the Russian Academy of Sciences, Chief Researcher of the Federal Research Center of Problems of Chemical Physics and Medicinal Chemistry RAS (FRC PCP MC RAS) (Chernogolovka, Russian Federation).

https://orcid.org/0000-0002-5541-5401

tolbin@inbox.ru

Alexander Yu. Gerasimenko, Dr. Sci. (Tech.), Professor in Institute of Biomedical Systems, National Research University of Electronic Technology – MIET (Zelenograd, Moscow, Russian Federation); Head of the Laboratory of Biomedical Nanotechnology, I. M. Sechenov First Moscow State Medical University (Moscow, Russian Federation).

https://orcid.org/0000-0001-6514-2411

gerasimenko@bms.zone

Received October 6, 2025; approved after reviewing November 6, 2025; accepted for publication November 7, 2025; published online September 25, 2026.